Ultrasonic study of the filled skutterudite compound $PrRu_4P_{12}$

Y. Nakanishi,* T. Kumagai, O. Masafumi, T. Tanizawa, and M. Yoshizawa
Graduate School of Frontier Materials Function Engineering, Iwate University, Morioka 020-8551, Japan

S. R. Saha,† H. Sugawara,‡ and H. Sato
Department of Physics, Tokyo Metropolitan University, Hachioji 192-0397, Japan
(Received 17 May 2005; revised manuscript received 17 January 2006; published 17 April 2006)

We have performed ultrasonic measurements of the filled skutterudite compound $PrRu_4P_{12}$ to investigate the elastic properties and the $4f$ electric state of Pr ions. A distinct feature associated with the metal-insulator transition was observed at T_{MI} of 62.3 K in the temperature dependence of the elastic constants C_{11}, $(C_{11}-C_{12})/2$, and C_{44}. These elastic constants increase monotonically with decreasing temperature below T_{MI}. However, a pronounced elastic softening toward low temperature was observed in C_{11}, $(C_{11}-C_{12})/2$, and C_{44} below around 20 K. We discuss the temperature development of the $4f$ electronic state of $PrRu_4P_{12}$ around T_{MI} and at low temperatures on the basis of the $4f$-level scheme formed by the crystalline electric field effect.

DOI: 10.1103/PhysRevB.73.165115 PACS number(s): 71.27.+a, 71.30.+h, 71.70.Ch, 75.10.Dg

I. INTRODUCTION

The filled skutterudite compounds RT_4X_{12} (R=rare earth, T=Fe, Ru, Os, and X=pnictogen) have been investigated intensively since the recent discovery of novel physical properties. In particular, the Pr compounds have attracted much attention from the viewpoint of anomalous nonmagnetic properties, indicating the importance of a quadrupolar degree of freedom.[1–6] In the case of conventional Pr compounds the hybridization strength is small enough to localize the $4f$ states owing to the contraction of the $4f$ wave function, compared with that of Ce and Yb compounds. In the filled skutterudite compounds, however, even in Pr compounds strongly correlated systems are realized due to a unique body-centered-cubic structure (space group $Im\,3$).[7,8] These systems provide us unique nonmagnetic stages with plural $4f$ electrons, quite different from those in Ce and Yb compounds. One of the essential ingredients in the physics is the strong hybridization between localized f electrons and conduction bands owing to the large coordination number of X to R. A metal-insulator (MI) transition observed in $PrRu_4P_{12}$ at T_{MI} of 62.3 K is one of the anomalous properties.[9] A clear anomaly was observed in the specific heat and thermal expansion coefficient measurement at T_{MI}.[10,11] The corresponding entropy was estimated to be around $R\ln 2$ below 20 K. However, no magnetic anomaly was observed in the magnetic susceptibility at T_{MI}. It is noted that the La substitution effect into the Pr site offers us significant information.[12] The magnetic susceptibility is almost temperature independent at low temperature at the Pr concentration less than around 50%, being indicative of nonmagnetic behavior (Van Vleck behavior), whereas a significant divergence toward low temperature was observed, more than 50%, being indicative of magnetic behavior (Curie-Weiss behavior). The magnetization studied by Tayama *et al.*, shows a sharp increase in low fields, implying ferromagnetic behavior. Furthermore, isotropic behavior was observed in the high-field magnetization curve.[13] The MI transition coincides with a structural phase transition that doubles the unit cell and opens a gap at the Fermi energy as reported by x-ray absorption near-edge spectroscopy XANES study and band calculation, respectively.[14–18] Recent neutron measurements done by Iwasa *et al.*, proposed $4f$ multiplets split by the crystalline electric field (CEF) effect for the Pr(1) and Pr(2) sites as follows:[19]

$$\Gamma_1(0)-\Gamma_4^{(2)}(95\ \mathrm{K})-\Gamma_{23}(108\ \mathrm{K})-\Gamma_4^{(1)}(184\ \mathrm{K}), \quad (1)$$

$$\Gamma_4^{(2)}(0)-\Gamma_1(26\ \mathrm{K})-\Gamma_{23}(140\ \mathrm{K})-\Gamma_4^{(1)}(222\ \mathrm{K}) \quad (2)$$

which are illustrated in detail later. This level scheme was determined at the lowest temperature of 5 K. Surprisingly, this level scheme depends strongly on the change of temperature. Although some models have been proposed, the ground state of the $4f$ electrons below the lowest temperature of the transition is still unsolved.

In this work, we have measured the elastic constants of $PrRu_4P_{12}$ by means of ultrasonic measurement in order to further investigate its ground state of $4f$ multiplets. The obtained results show a distinct feature in all elastic constants at T_{MI}, and a pronounced softening toward low temperature in C_{11}, $(C_{11}-C_{12})/2$, and C_{44}. The present results are explained reasonably by the proposed $4f$-level scheme of Pr ions determined by the recent inelastic neutron scattering measurement. We discuss the ground state properties and analyze them in comparison with other physical properties of $PrRu_4P_{12}$.

II. EXPERIMENT

The $PrRu_4P_{12}$ sample used in this work was grown by the tin-flux method. The starting materials were 3N (99.9% pure) Pr, 4N Ru, 6N P, and 5N Sn. The single crystal nature was confirmed by the back-reflection Laue technique. The elastic constants (C_{ij}) were measured by an ultrasonic apparatus based on a phase comparison method. The plates of quartz and $LiNbO_3$ transducers for the generation and detection of the sound waves with frequencies 5–15 MHz were used. They were glued on the parallel planes of the sample by the

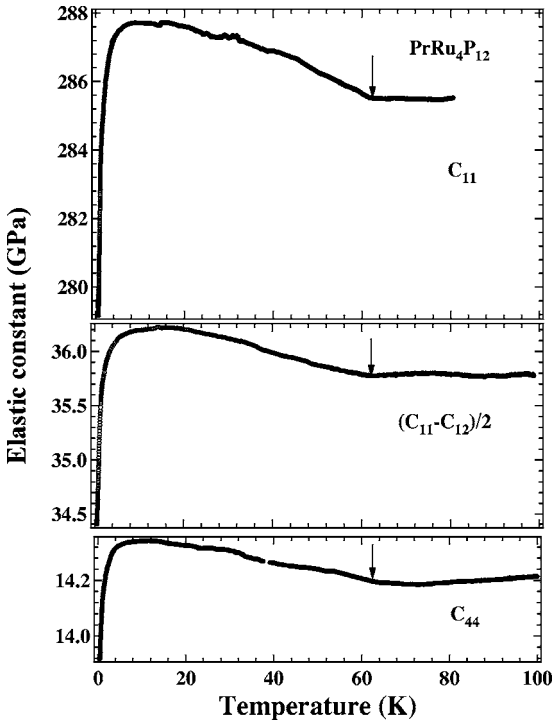

FIG. 1. Temperature dependence of elastic constants C_{11}, $(C_{11}+C_{12})/2$, and C_{44} of $PrRu_4P_{12}$. Downward arrows indicate the metal-insulator transition temperature T_{MI}.

elastic polymer Thiokol. The specimen used in this study has a size of 1.4 and 1.5 mm for the ⟨100⟩ and the ⟨110⟩ axis, respectively. In the estimation of the elastic constant $C=\rho v^2$, we used the mass density $\rho=5.836$ g/cm^3 for $PrRu_4P_{12}$ with a lattice parameter $a=8.0516$ Å.

III. EXPERIMENTAL RESULTS

Figure 1 shows the temperature dependence of elastic constants C_{11}, $(C_{11}-C_{12})/2$, and C_{44} of $PrRu_4P_{12}$. C_{11} is the elastic constant determined by the longitudinal sound wave propagated along the ⟨100⟩ axis. $(C_{11}-C_{12})/2$ and C_{44} are those determined by the transverse one propagated along ⟨100⟩ with the polarization parallel to ⟨010⟩ and propagated along ⟨110⟩ with the polarization parallel to $\langle 1\bar{1}0\rangle$, respectively. We used a longitudinal sound wave with a frequency of 10 MHz for the measurement of C_{11} and transverse waves of 5 and 15 MHz for $(C_{11}-C_{12})/2$ and C_{44}, respectively. A distinct bend was observed at T_{MI} as indicated by arrows, and these elastic constants increase monotonically below T_{MI}. Furthermore, a pronounced elastic softening toward low temperature appears in C_{11}, $(C_{11}-C_{12})/2$, and C_{44}. It is likely that the softening toward low temperature still continues in the temperature range below 0.5 K. The absolute values of each elastic constant, calculated bulk modulus $C_B=(C_{11}+2C_{12})/3$, and Poisson ratio $\gamma=C_{12}/(C_{11}+C_{12})$ from C_{11} and $(C_{11}-C_{12})/2$ at both 77 and 4.2 K are listed in Table I. Figure 2 shows the temperature dependence of C_{11} under selected fields along the ⟨100⟩ axis. In some cases, the offsets of data are shifted arbitrarily to avoid overlap of curves,

TABLE I. The absolute values of each elastic constant and bulk modulus $C_B=(C_{11}+2C_{12})/3$ and Poisson ratio $\gamma=C_{12}/(C_{11}+C_{12})$ at both 77 and 4.2 K.

Mode	Elastic constant	
	at 4.2 K	at 77 K
C_{11}	230 GPa	225 GPa
$(C_{11}-2C_{12})/2$	27.5 GPa	27.0 GPa
C_{44}	17.7 GPa	17.4 GPa
$C_B=(C_{11}+2C_{12})/3$	193.5 GPa	188.9 GPa
$\gamma=C_{12}/(C_{11}+C_{12})$	0.432(1)	0.438(1)

hereafter. The pronounced softening toward low temperature is gradually suppressed with increasing field. The softening is undetectable above 5 T. Figure 3 shows the temperature dependence of $(C_{11}-C_{12})/2$ under selected fields along the ⟨110⟩ axis. Similarly, a pronounced softening toward low temperature is gradually suppressed with increasing field. The softening is undetectable above 5 T. The temperature dependence of C_{44} under selected fields along the ⟨100⟩ axis is shown in Fig. 4. It is also suppressed with increasing field. The softening is undetectable above 5 T. It is noted that the softening of C_{44} begins below around 1.5 K in zero field, different from that of C_{11} and $(C_{11}-C_{12})/2$ in which the softening begins below around 18 K. These results share certain similarities in that the characteristic softening toward low temperature is undetectable under a field above around 5 T. The origin of the elastic softening observed in C_{11}, $(C_{11}-C_{12})/2$, and C_{44} will be analyzed and discussed in detail later. Figure 5 shows the temperature dependence of $(C_{11}-C_{12})/2$ in selected fields along the ⟨110⟩ axis around the metal-insulator transition temperature in a precise scale. The clear bend behavior gradually becomes smeared with increasing field. It is highly marked that the bend hardly shifts with increasing field. The inset of Fig. 5 shows the

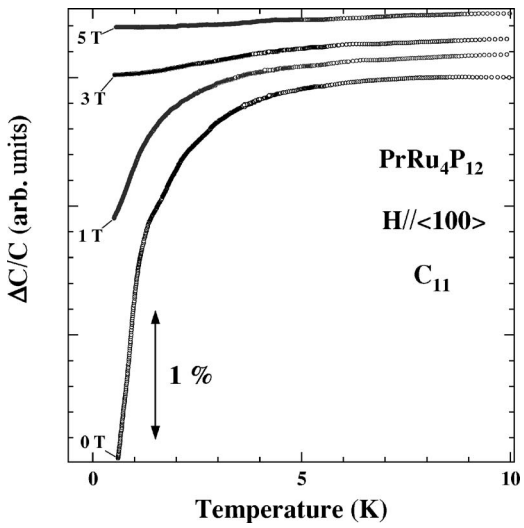

FIG. 2. Temperature dependence of C_{11} in selected magnetic fields along the ⟨100⟩ axis. Their offsets are shifted arbitrarily to avoid overlap of the curves.

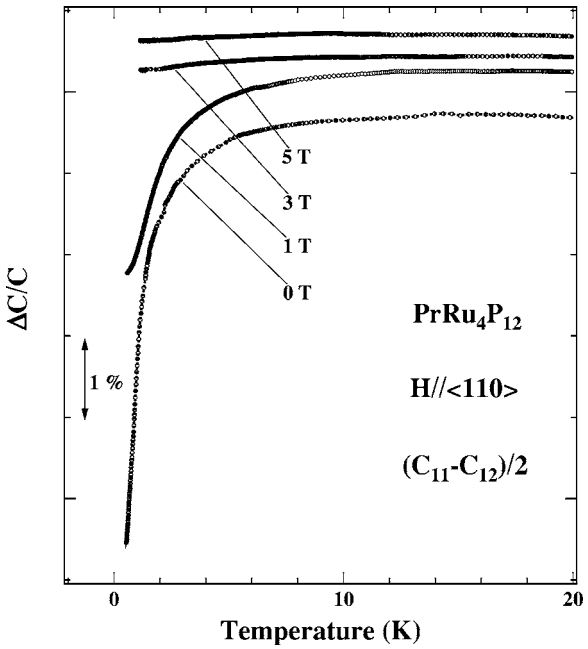

FIG. 3. Temperature dependence of $(C_{11}-C_{12})/2$ in selected magnetic fields along the ⟨110⟩ axis. Their offsets are shifted arbitrarily to avoid overlap of the curves.

magnetic phase diagram of $PrRu_4P_{12}$ determined by the present results in a field for $H\|\langle 100\rangle$ and for $H\|\langle 110\rangle$ deduced from C_{11}, C_{44}, and $(C_{11}-C_{12})/2$, respectively. The phases I and II correspond to the metallic and nonmetallic phases, respectively. The MI transition temperature T_{MI} is almost independent of magnetic field, which is consistent with those determined by the other physical properties such as specific heat and magnetic susceptibility. This boundary shows almost isotropic behavior. It is noted that all of these

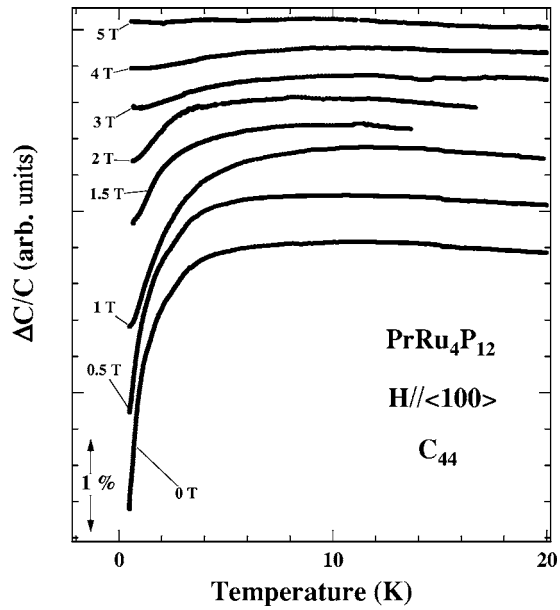

FIG. 4. Temperature dependence of C_{44} in selected magnetic fields along the ⟨100⟩ axis. Their offsets are shifted arbitrarily to avoid overlap of the curves.

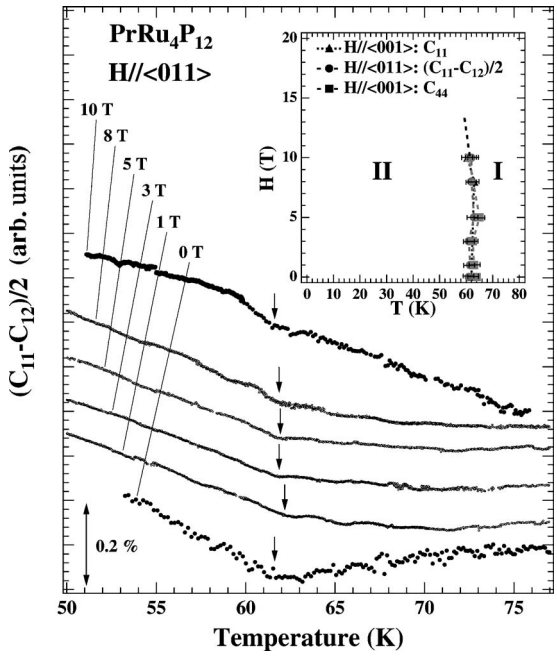

FIG. 5. Temperature dependence of $(C_{11}-C_{12})/2$ in selected fields along the ⟨110⟩ axis around the T_{MI} temperature in a precise scale. Their offsets are shifted arbitrarily to avoid overlap of the curves. Inset shows the magnetic phase diagram of $PrRu_4P_{12}$ under a field along the ⟨100⟩ and the ⟨110⟩ axes determined by C_{11}, C_{44}, and $(C_{11}-C_{12})/2$, respectively. They are indicated by the closed triangles, closed circles, and closed squares, respectively.

elastic constants are almost constant above T_{MI}, whereas they increase monotonically in the nonmetallic phase, i.e., below T_{MI}. This feature will also be discussed in detail later.

IV. DISCUSSION

Here, we discuss the origin of the observed elastic softening. First, we consider the quadrupolar interaction between Γ_3 type and Γ_5 type quadrupolar moments associated with the softening observed in the transverse $(C_{11}-C_{12})/2$ mode and C_{44} mode, respectively. According to the effective Hamiltonian with respect to the quadrupolar moment for the $4f$ electron, $\mathcal{H}_{qs}$ for interaction of the quadrupolar moment O_Γ in the $4f$ electronic state with the local strain ϵ_Γ induced by a sound wave and $\mathcal{H}_{qq}$ for the intersite quadrupolar interaction are described as follows:[20–22]

$$\mathcal{H}_{qs} = \sum_i g_\Gamma O_\Gamma(i)\epsilon_\Gamma, \tag{3}$$

$$\mathcal{H}_{qq} = \sum_i g'_\Gamma \langle O_\Gamma\rangle O_\Gamma(i), \tag{4}$$

where $O_\Gamma(i)$ is the equivalent quadrupolar operator at the ith Pr site and g_Γ (Γ denotes the irreducible representation of the point group, i.e., Γ_3 and Γ_5) is the coupling constant. g'_Γ is the quadrupolar coupling constant and $\langle O_\Gamma\rangle$ is the mean field of the quadrupolar moment.

The Hamiltonian used to describe the elastic properties of the present system is written including the above terms as follows:

$$\mathcal{H}_{total} = \mathcal{H}_{CEF} + \mathcal{H}_{Zeeman} + \mathcal{H}_{qs} + \mathcal{H}_{qq} \tag{5}$$

where the magnetic interaction among the Pr sites is neglected for simplicity. In fact no magnetic transition has been observed in the temperature range down to 0.5 K.[23] For this reason, we neglect any Pr-Pr interactions in the analysis. $\mathcal{H}_{CEF}$ is the cubic crystalline electric field term with T_h site symmetry described as follows:

$$\mathcal{H}_{CEF} = W\left[x\left(\frac{O_4}{F(4)}\right) + (1-|x|)\left(\frac{O_6^c}{F(6)}\right) + y\left(\frac{O_6^t}{F^t(6)}\right)\right]. \tag{6}$$

The descriptions follow the Takegahara formula, where $O_4 = O_4^0 + 5O_4^4$, $O_6^c = O_6^0 - 21O_6^4$, $O_6^t = O_6^2 - O_6^6$ by using the Stevens' operators, and $F(4)=60$, $F(6)=2560$, $F^t(6)=240$.[8] Here we use the proposed CEF parameters $x=-0.254$, $y=0.009$, and $W=0.14$ meV for Pr(1) and $x=0.580$, $y=0.073$, and $W=0.364$ meV for Pr(2) at 5 K, and $x=-0.189$, $y=0.021$, and $W=0.129$ meV for Pr(1) and $x=0.582$, $y=0.122$, and $W=0.238$ meV for Pr(2) at 20 K determined by the recent inelastic neutron scattering measurement.[19] $\mathcal{H}_{Zeeman}$ is the Zeeman coupling with the applied magnetic field **H** and the total angular momentum **J** described as follows:

$$\mathcal{H}_{Zeeman} = -g_J \mu_B \mathbf{J} \cdot \mathbf{H} \tag{7}$$

where g_J and μ_B are the Landé g factor and Bohr magneton, respectively. The temperature dependence of the symmetric elastic constant C_Γ is described as

$$C_\Gamma(T) = C_\Gamma^{(0)}(T) - \frac{N g_\Gamma^2 \chi_\Gamma^{(s)}(T)}{1 - g_\Gamma' \chi_\Gamma^{(s)}(T)} \tag{8}$$

where N denotes the number of Pr ions in unit volume, and $C_\Gamma^{(0)}$ and $\chi_\Gamma^{(s)}(T)$ denote the background without quadrupolar-strain interaction and the charge susceptibility, respectively. If we neglect the intersite quadrupolar interactions g_Γ' between Pr ions, the elastic constant is simply described as $C_\Gamma(T) = -N g_\Gamma^2 \chi_\Gamma^{(s)}(T)$ as used below for the calculations. $\chi_\Gamma^{(s)}(T)$ is described in a cubic CEF potential as

$$\chi_\Gamma^{(s)}(T) = \sum_{ik} \frac{\exp(-E_{ik}^{(0)}/k_B T)}{Z}\left(\frac{1}{k_B T}|\langle ik|O_\Gamma|ik\rangle|^2 - 2\sum_{jl}\frac{|\langle ik|O_\Gamma|jl\rangle|^2}{E_i - E_j}\right) \tag{9}$$

where $|ik\rangle$ and Z represent the kth eigenfunction of the ith CEF level and the partition function, respectively. In second-order perturbation theory with respect to the Hamiltonians $\mathcal{H}_{Zeeman}$ and $\mathcal{H}_{qs}$, one obtains the free energy with respect to the elastic strain ϵ_Γ. From the second derivative of the obtained free energy, the temperature dependence of the charge susceptibility $\chi^{(s)}$ is determined. If the ground state is degenerate with respect to a quadrupolar moment O_Γ, a softening in the corresponding elastic constant is expected to occur due to the nonzero Curie term i.e., the first term in Eq. (9).

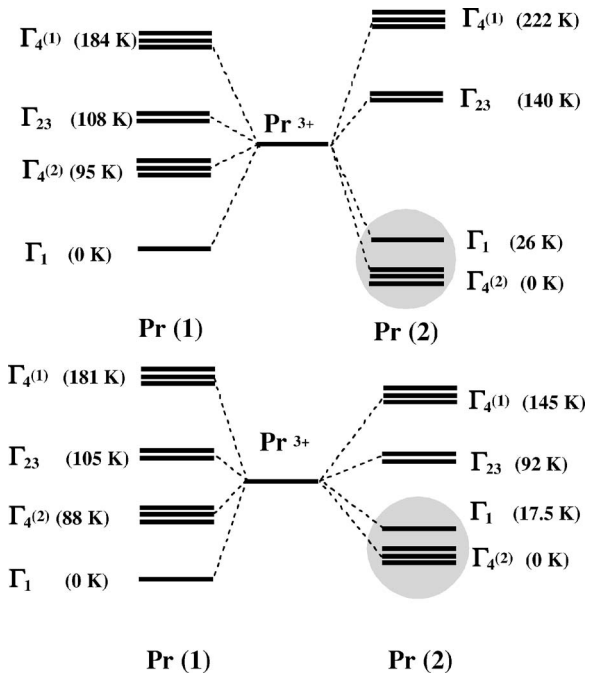

FIG. 6. The proposed model of the level scheme of the 4*f* electronic state of $PrRu_4P_{12}$ for each of two inequivalent Pr sites (top) at 5 K and (bottom) at 20 K for $H=0$ (Ref. 19).

Let us come back to the ground state properties. The $\Gamma_4^{(1)}$ and $\Gamma_4^{(2)}$ triplet possesses both Γ_3 and Γ_5 type quadrupolar moments. So if either state is the ground state or locates close to the ground state in energy, a softening toward low temperature is expected in both $(C_{11}-C_{12})/2$ and C_{44}. If one uses the CEF level scheme proposed by the inelastic neutron scattering measurement, a remarkable softening should be observed in both $(C_{11}-C_{12})/2$ and C_{44}. As mentioned in the Introduction, there are two different sites for Pr ions with a different site symmetry below T_{MI}.[14–16] Furthermore, it is reported that the CEF level scheme is strongly dependent on change of temperature.[19] Figure 7 shows the calculated temperature dependence of the charge susceptibilities $\chi_{\Gamma 3}^{(s)}(T)$ and $\chi_{\Gamma 5}^{(s)}(T)$ for each Pr site in selected magnetic fields based on the formula (9) with the proposed level scheme at 5 K as shown in Fig. 6, where again the charge susceptibilities $\chi_{\Gamma 3}^{(s)}(T)$ and $\chi_{\Gamma 5}^{(s)}(T)$ contribute predominantly to the elastic constants $(C_{11}-C_{12})/2$ and C_{44}, respectively, as mentioned above. While the calculated elastic constant for Pr(1) site shows almost temperature-independent behavior, that for the Pr(2) site shows a characteristic softening toward low temperature. Furthermore, the latter contribution reasonably reproduces the experimental results even in a magnetic field. These results strongly suggest that the Pr(2) sites, that is, $\Gamma_4^{(2)}$, are responsible for the obtained softening toward low temperatures.

Next, let us discuss the field dependence of elastic constants at selected temperatures. Since the CEF level scheme is strongly dependent on temperature, especially below T_{MI}, it may be an appropriate way to obtain significant information regarding the level scheme. Figure 8 shows the field

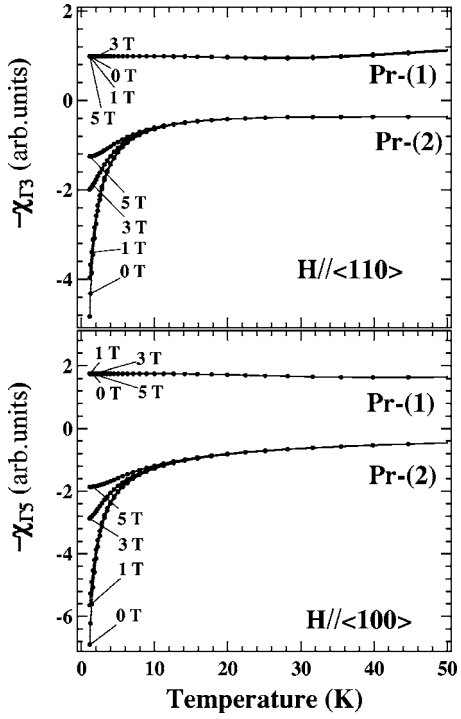

FIG. 7. Theoretical results of the temperature dependence of (top) charge susceptibilities $\chi_{\Gamma 3}$ and (bottom) $\chi_{\Gamma 5}$ in selected magnetic fields along the ⟨100⟩ and the ⟨110⟩ axes, respectively, for each different Pr site (1) and (2). Their offsets are shifted arbitrarily to avoid overlap of the curves.

dependence of elastic constants $(C_{11}-C_{12})/2$ and C_{44} at 5 K, and their corresponding calculated results. The calculated results of the charge susceptibility $\chi^{(s)}_{\Gamma 3}(T)$ and $\chi^{(s)}_{\Gamma 5}(T)$ are shown for each Pr site (1) and (2) in the middle and bottom panels, respectively. The charge susceptibilities, namely, the elastic constants $(C_{11}-C_{12})/2$ and C_{44} have a slight minimum around 1 T and then exhibit a concave curvature in a magnetic field above 2 T. While the calculated elastic constant for the Pr(1) site shows almost field-independent behavior, that for the Pr(2) site shows a slight convex curvature in low fields and a concave one above around 2 T which is in good agreement with the experimental result of both $(C_{11}-C_{12})/2$ and C_{44}. Figure 9 shows the field dependence of elastic constants $(C_{11}-C_{12})/2$, and C_{44} at 20 K, and their corresponding calculated results. Although the characteristic features were not observed, they increase monotonically with increasing field. Similarly to those at 5 K, the calculated result for the Pr(2) site reproduces roughly the experimental results for both elastic constants $(C_{11}-C_{12})/2$ and C_{44} at 20 K.

A comparison of the experimental results and the calculated ones based on the CEF effect indicates that $\Gamma_4^{(2)}$ plays an important role to cause the characteristic softening toward low temperatures observed in C_{11}, $(C_{11}-C_{12})/2$, and C_{44}, and the present results are consistent with those of the inelastic neutron scattering measurement.[19] Again, a clear crystal field spectrum was evidently observed in $PrRu_4P_{12}$, indicating that the ground states $\Gamma_4^{(2)}$ and Γ_1 should play a crucial role at low temperatures. By contrast, a quasielastic scattering with a broad linewidth was observed in $PrFe_4P_{12}$ in which the elastic constants cannot be explained reasonably only by the proposed CEF level scheme model.[24–28] This

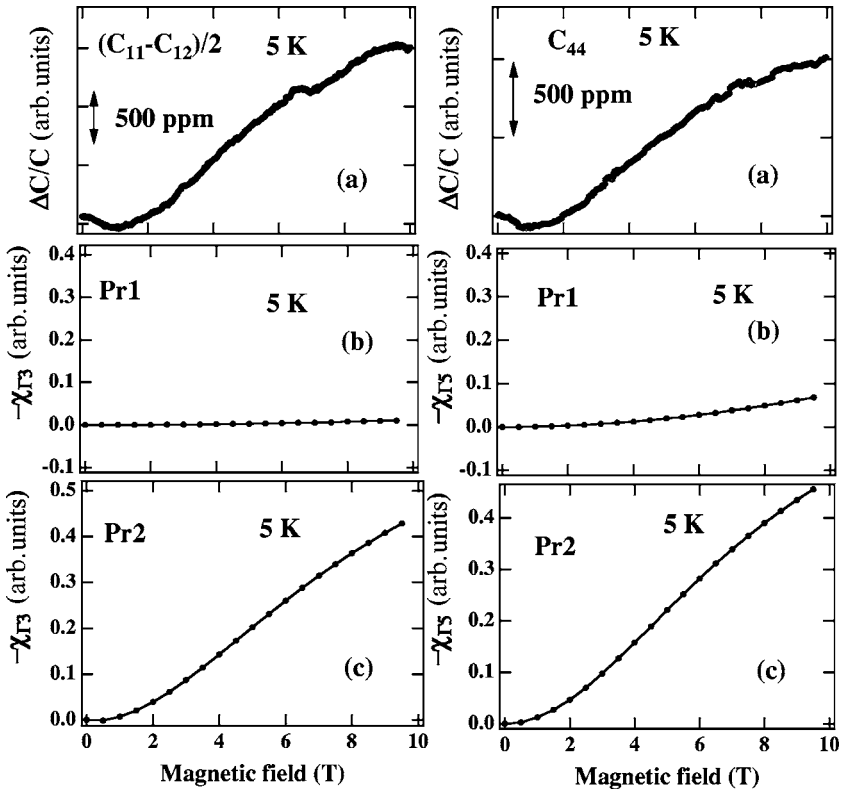

FIG. 8. Left: (a) Experimental and (b), (c)theoretical results of magnetic field dependence of $(C_{11}-C_{12})/2$ along the ⟨110⟩ axis at 5 K. Right: (a) Experimental and (b), (c) theoretical results of magnetic field dependence of C_{44} along the ⟨100⟩ axis at 5 K.

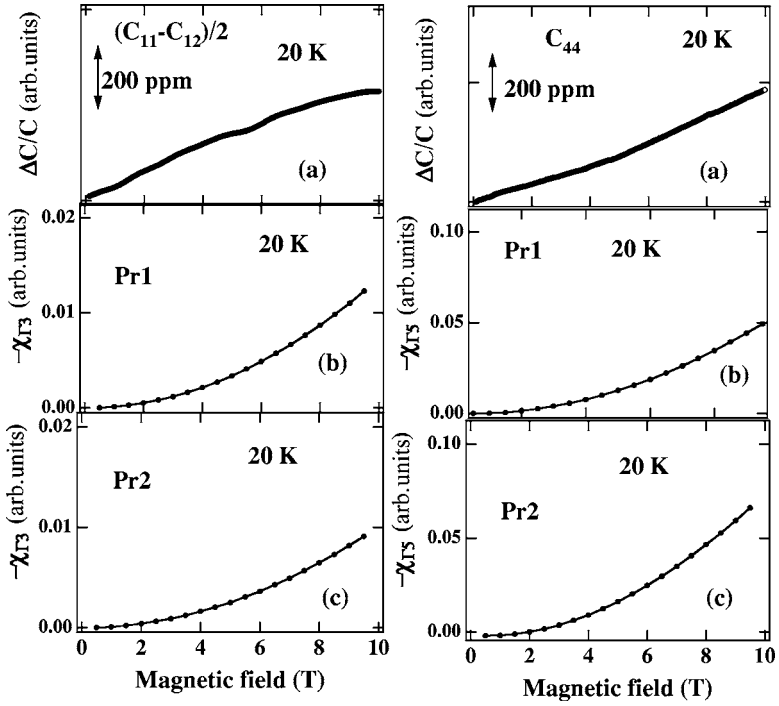

FIG. 9. Left: (a) Experimental and (b), (c) theoretical results of magnetic field dependence of $(C_{11}-C_{12})/2$ along the $\langle 110\rangle$ axis at 20 K. Right: (a) Experimental and (b), (c) theoretical results of magnetic field dependence of C_{44} along the $\langle 100\rangle$ axis at 20 K.

high contrast is probably ascribable to the role of conduction electrons.

Apart from the CEF effect let us discuss the origin of the elastic softening toward low temperature. There are two other main possibilities to cause the characteristic softening. One is the coupling between enhanced bands and the relevant elastic strains. If carriers with heavy mass form the Fermi surface this effect can be important in causing softening.[29–33] This scenario is likely to be seen in other filled skutterudite compounds such as $SmRu_4P_{12}$ and $CeOs_4Sb_{12}$ at low temperatures. We do not rule out this scenario to explain the present elastic softening toward low temperatures observed in C_{11}, $(C_{11}-C_{12})/2$, and C_{44}. In $PrRu_4P_{12}$ metal-insulator transition occurs below 62.3 K, leading to a state at low temperatures in which this contribution would not be so strong. The temperature to begin the characteristic softening is different between $(C_{11}-C_{12})/2$ and C_{44}, which is not expected in the present CEF model. As seen in $CeOs_4Sb_{12}$, a steep decrease of the elastic constant at low temperatures may be due to the different magnitude of the coupling constant between the elastic strain and a relevant order parameter.

Another possibility is the quantum "rattling" effect recently proposed by Goto *et al.*[34–36] However, this effect is observed at much lower temperatures and in an extremely small amount. In $La_3Pd_{20}Ge_6$ a slight softening is observed below 2 K as reported by Nemoto *et al.*[34] Furthermore, they suggest that the quantum rattling effect plays an important role in $PrOs_4Sb_{12}$.[35,36] However, since the characteristic dispersion of the elastic constants has not been observed in $PrRu_4P_{12}$, this scenario seems to be not suitable to explain the observed softening toward low temperatures in the present case.

Here, let us discuss the distinct bend observed at T_{MI} in all elastic constants. As already reported in $SmRu_4P_{12}$, a decrease of the carrier number influences the elastic anomaly.[29,37] According to the long wave limit of the Lindhard function, a decrease in the density of states at the Fermi energy causes an increase of the elastic constant. This is a standard behavior of the elastic constant at the MI transition.[29,38,39] On the other hand, this observed bend at T_{MI} provides us another important meaning. Even in compounds with a quadrupolar transition at high temperatures such as DyB_2C_2, a characteristic softening toward the transition temperature was observed.[40] The absence of elastic softening toward T_{MI} indicates that this transition has nothing to do with the quadrupolar transition. That is to say, the degeneracy of quadrupolar moments still remains below T_{MI}. Thus, the $4f$ electronic state does not contribute directly to this metal-insulator transition, including the experimental fact that the magnetic moment does not contribute to it either. These facts imply that the band, i.e., Fermi surface plays a crucial role to bring about this transition, consistent with the de Haas–van Alphen measurement.[41]

Finally, we would like to make a comment on the proposed CEF level scheme obtained by inelastic neutron scattering measurement.[19] If the $\Gamma_4^{(2)}$ triplet is the ground state in this system, a magnetic phase transition is expected since $\Gamma_4^{(2)}$ has a magnetic moment. Down to 0.5 K no magnetic transition has been reported so far. The extremely low concentration of carriers and existence of two different Pr sites in the system at low temperatures might suppress the magnetic exchange interaction, so to speak, the Ruderman-Kittel-Kasuya-Yosida interactions.

V. CONCLUDING REMARKS

In this paper we presented the elastic properties of $PrRu_4P_{12}$. The elastic constants C_{11}, $(C_{11}-C_{12})/2$, and C_{44} exhibit a distinct bend at T_{MI}. This is probably ascribed to a

decrease of density of states at the Fermi level and the resultant decrease of the carrier numbers. A pronounced softening toward low temperatures was observed in C_{11} and $(C_{11}-C_{12})/2$ below 20 K and C_{44} below 2 K. The obtained characteristic softening toward low temperatures is explained reasonably on the basis of the proposed $4f$-level scheme: mainly $\Gamma_{(1)}$-$\Gamma_4^{(2)}$ and $\Gamma_4^{(2)}$-$\Gamma_{(1)}$ pseudoquartet states. That is to say, the pseudoquartet states essentially play a crucial role in the low-temperature properties of the $PrRu_4P_{12}$ system. The same measurements at temperature below 0.5 K are currently in progress by means of a ^{3}He-^{4}He diluted refrigerator. Furthermore, the investigation of elastic properties on $Pr_xLa_{1-x}Ru_4P_{12}$ system in which the nonmagnetic element La is substituted on the Pr site are required to determine the explicit CEF level scheme of Pr ion, and we are planning to do that in the near future.

ACKNOWLEDGMENTS

The authors thank M. Nakamura for support in the experiments. The measurements have been performed in the Cryogenic Division of the Center for Instrumental Analysis, Iwate University. This work was supported by a Grant-in-Aid for Science Research Priority Area "Skutterudite" (No. 15072202) of the Minister of Education, Culture, Sports, Science, and Technology of Japan.

*Electronic address: yoshiki@iwate-u.ac.jp
†Present address: Institute of Material Structure Science, National Laboratory for High Energy Physics (KEK), Tsukuba 305-0801, Japan.
‡Present address: Faculty of Integrated Arts and Sciences, The University of Tokushima, Tokushima 770-8502, Japan.

[1] H. Sato, Y. Abe, H. Okada, T. D. Matsuda, K. Abe, H. Sugawara, and Y. Aoki, Phys. Rev. B **62**, 15125 (2000).
[2] Y. Aoki, T. Namiki, T. D. Matsuda, K. Abe, H. Sugawara, and H. Sato, Phys. Rev. B **65**, 064446 (2002).
[3] H. Sugawara, T. D. Matsuda, K. Abe, Y. Aoki, H. Sato, S. Nojiri, Y. Inada, R. Settai, and Y. Ônuki, Phys. Rev. B **66**, 134411 (2002).
[4] E. D. Bauer, N. A. Frederick, P.-C. Ho, V. S. Zapf, and M. B. Maple, Phys. Rev. B **65**, 100506(R) (2002).
[5] H. Sugawara, S. Osaki, S. R. Saha, Y. Aoki, H. Sato, Y. Inada, H. Shishido, R. Settai, Y. Ônuki, H. Harima, and K. Oikawa, Phys. Rev. B **66**, 220504(R) (2002).
[6] Y. Aoki, T. Namiki, S. Ohsaki, S. R. Saha, H. Sugawara, and H. Sato, J. Phys. Soc. Jpn. **71**, 2098 (2002).
[7] W. Jeitschko and D. Braun, Acta Crystallogr., Sect. B: Struct. Crystallogr. Cryst. Chem. **33**, 340 (1977).
[8] K. Takegahara, H. Harima, and A. Yanase, J. Phys. Soc. Jpn. **70**, 1190 (2001).
[9] C. Sekine, T. Uchiumi, I. Shirotani, and T. Yagi, Phys. Rev. Lett. **79**, 3218 (1997).
[10] C. Sekine, T. Inaba, I. Shirotani, M. Yokoyama, H. Amitsuka, and T. Sakakibara, Physica B **281&282**, 303 (2000).
[11] K. Matsuhira, T. Tkikawa, T. Sakakibara, C. Sekine, and I. Shirotani, Physica B **281&282**, 298 (2000).
[12] C. Sekine, T. Inaba, K. Kihou, and I. Shirotani, Physica B **281&282**, 300 (2000).
[13] T. Tayama *et al.*, Phys. Rev. B (to be published).
[14] C. H. Lee, H. Oyanagi, C. Sekine, I. Shirotani, and M. Ishii, Phys. Rev. B **60**, R13253 (1999).
[15] C. H. Lee, H. Matsuhara, A. Yamamoto, T. Ohta, H. Takazawa, K. Ueno, C. Sekine, I. Shirotani, and T. Hirayama, J. Phys.: Condens. Matter **13**, L45 (2001).
[16] C. H. Lee, H. Matsuhara, H. Yamaguchi, C. Sekine, K. Kihou, T. Suzuki, T. Noro, and I. Shirotani, Phys. Rev. B **70**, 153105 (2004).
[17] H. Harima and K. Takegahara, Physica B **312-313**, 843 (2002).
[18] H. Harima, K. Takegahara, K. Ueda, and S. H. Curnoe, Acta Phys. Pol. B **34**, 1189 (2003).
[19] K. Iwasa *et al.*, Physica B **359**, 833 (2002).
[20] S. Nakamura, T. Goto, S. Kunii, K. Iwashita, and A. Tamaki, J. Phys. Soc. Jpn. **63**, 623 (1994).
[21] P. M. Levy, J. Phys. C **6**, 3545 (1973).
[22] V. Dohm and P. Fulde, Z. Phys. B **21**, 369 (1975).
[23] G. P. Meisner, Physica B & C **108B**, 763 (1981).
[24] L. Hao, K. Iwasa, M. Nakajima, D. Kawana, K. Kuwahara, M. Kohgi, H. Sugawara, T. D. Matsuda, Y. Aoki, and H. Sato, Acta Phys. Pol. B **34**, 1113 (2003).
[25] K. Iwasa, L. Hao, M. Nakajima, M. Kohgi, H. Sugawara, Y. Aoki, H. Sato, and T. D. Matsuda, Acta Phys. Pol. B **34**, 1117 (2003).
[26] Y. Nakanishi, T. Shimizu, M. Yoshizawa, T. D. Matsuda, H. Sugawara, and H. Sato, Phys. Rev. B **66**, 134411 (2002).
[27] Y. Nakanishi, M. Yoshizawa, T. Yamaguchi, H. Hazama, Y. Nemoto, T. Goto, T. D. Matsuda, H. Sugawara, and H. Sato, J. Phys.: Condens. Matter **14**, L715 (2002).
[28] Y. Nakanishi, M. Yoshizawa, T. Yamaguchi, H. Hazama, Y. Nemoto, T. Goto, T. D. Matsuda, H. Sugawara, and H. Sato, Acta Phys. Pol. B **34**, 1079 (2003).
[29] Y. Yoshizawa, Y. Nakanishi, T. Kumagai, M. Oikawa, C. Sekine, and I. Shirotani, J. Phys. Soc. Jpn. **73**, 315 (2004).
[30] Y. Nakanishi *et al.*, Physica B (to be published).
[31] B. Lüthi, J. Magn. Magn. Mater. **52**, 70 (1985).
[32] P. Thalmeier, J. Magn. Magn. Mater. **76&77**, 299 (1988).
[33] S. Nakamura, T. Goto, Y. Ishikawa, S. Sakatsume, and M. Kasuya, J. Phys. Soc. Jpn. **60**, 2305 (1991).
[34] Y. Nemoto, T. Yamaguchi, T. Horino, M. Akatsu, T. Yanagisawa, T. Goto, O. Suzuki, A. Dönni, and T. Komatsubara, Phys. Rev. B **68**, 184109 (2003).
[35] T. Goto, Y. Nemoto, T. Yamaguchi, M. Akatsu, T. Yanagisawa, O. Suzuki, and H. Kitazawa, Phys. Rev. B **70**, 184126 (2004).
[36] T. Goto, Y. Nemoto, K. Sakai, T. Yamaguchi, M. Akatsu, T. Yanagisawa, H. Hazama, K. Onuki, H. Sugawara, and H. Sato, Phys. Rev. B **69**, 180511 (2004).
[37] Y. Nakanishi (unpublished).
[38] J. Mayers, Phys. Rev. B **41**, 41 (1990).
[39] K. Maki and A. Virosztek, Phys. Rev. B **36**, 2910 (1987).
[40] Y. Nemoto, T. Yanagisawa, K. Hyodo, T. Goto, S. Miyata, R. Watanuki, and K. Suzuki, Physica B **329-333**, 641 (2003).
[41] S. R. Saha, H. Sugawara, Y. Aoki, H. Sato, Y. Inada, H. Shishido, R. Settai, Y. Onuki, and H. Harima, Phys. Rev. B **71**, 132502 (2005).